Mesh antennas for dual polarization

SUZUKI, N. / YAMAUCHI, J. / ISHII, T. / NAKANO, H.

Mesh Antennas for Dual Polarization

H. Nakano, *Fellow, IEEE*, N. Suzuki, T. Ishii, and J. Yamauchi, *Member, IEEE*

Abstract—**Three mesh antennas, all having an extremely small antenna height of approximately 0.06 wavelength above a ground plane, are presented. First, a mesh antenna excited with a balanced feed is analyzed. It is revealed that the mesh antenna radiates a linearly polarized wave with no cross-polarization component in the principal planes. The radiation mechanism is explained using the current distribution. Second, a mesh antenna excited with an unbalanced feed is analyzed. This antenna shows almost the same radiation characteristics as the mesh antenna with a balanced feed. The frequency bandwidth for a VSWR = 2 criterion is evaluated to be approximately 3%. Third, a mesh antenna having two perturbation elements is analyzed. It is found that the antenna acts as a radiation element of circular polarization. The frequency bandwidth for a 3-dB axial ratio criterion is calculated to be approximately 1%. The mesh antennas in the first and second analyses can be used as dual linear polarization elements by appropriately switching the feed. Similarly, the mesh antenna in the third analysis can be used as a dual circular polarization element by switching the feed.**

Index Terms—**Circular polarization, dual polarization, linear, wire antenna.**

I. INTRODUCTION

A LOOP antenna is a fundamental radiation element [1]–[4], which is usually made of a conducting wire and located in free space. Recently, loops printed on a dielectric substrate have been analyzed [5], [6]. The analysis has shown that the loop can radiate both linearly polarized [5] and circularly polarized [6] waves.

This paper presents a mesh antenna, which is regarded as an extension of the loop antenna. The purpose of this paper is to investigate the radiation characteristics of the mesh antenna as a dual linearly polarized antenna and a dual circularly polarized antenna.

The prototype of the mesh antenna is composed of a square loop $ABCD$ and four wires added to the loop, as shown in Fig. 1(a). This antenna is excited from the center region of the antenna with a balanced feed. The antenna is designated as the mesh antenna with balanced feed (MA-B). First, the MA-B is analyzed by using the method of moments (MoM) [7], [8]. A limitation of the MoM is brought to light in its application to an integral equation derived for a thin wire antenna [9]. The MoM analysis shows that the MA-B radiates a linearly x- or y-polarized wave.

Secondly, the MA-B is simplified to the antenna shown in Fig. 1(b), which does not require a balanced feed. This antenna is designated as the mesh antenna with unbalanced feed (MA-U). The MA-U has two input terminals: one is fed and the other is left open-circuited. The MoM is again used to analyze the MA-U. The

antenna input impedance as a function of the location of a feed point is investigated and illustrated with a voltage standing-wave ratio (VSWR) curve, to obtain impedance matching to a 50-Ω line. It is found that the MA-U has radiation characteristics similar to the MA-B, and the MA-U can act as a dual linearly polarized radiation element by selecting the feed point.

Thirdly, a radiation element of dual circular polarization based on the MA-U is considered. Two perturbation elements are added to the MA-U to form a circularly polarized wave. This radiation element is designated as the MA-U with perturbation elements [MA-UP; see Fig. 1(c)]. MoM analysis shows that the current along the square periphery (loop) flows as a traveling wave, which contributes to radiation of a circularly polarized wave. The frequency responses for the axial ratio, VSWR, and gain are presented, together with measured results. Some comments on the perturbation elements are made to explain the antenna characteristics.

The MA-U and MA-UP have simple feed systems without balun circuits. In addition, these antennas have a very low-profile structure (the mesh above a ground plane is approximately 0.06 wavelength). Therefore, the antennas are suitable, for example, for automobile rooftop telecommunication antennas.

II. NUMERICAL ANALYSIS

The antennas under analysis are shown in Fig. 1(a)–(c). A conducting plane (ground plane) backs the horizontal mesh wires in each antenna. A dielectric material of relative permittivity $\varepsilon_r \approx 1$ (honeycomb material) is used as a spacer between the ground plane and the mesh wires. The ground plane is of infinite extent, and hence image theory is used for the analysis.

To obtain the current distribution along the antenna conductor, the MoM [7], [8] is applied to an integral equation derived for an arbitrarily shaped thin wire [9], whose radius ρ satisfies $\rho \ll$ wavelength (ρ is usually selected to be less than 0.01 wavelength). In this paper, the wire radius is fixed to be $\rho = 0.002\lambda_0$, where λ_0 is the free-space wavelength at a test frequency of 4 GHz. The kernel of the equation is expressed in closed form after the thin wire is subdivided into numerous segments, each being regarded as linear. The length of each segment is always chosen to be greater than 2.5ρ. This choice gives good convergence of the current distribution. In other words, the relationship between the length and radius of each segment limits the application of the MoM to the integral equation. Note that piecewise sinusoidal functions are adopted for the expansion and weighting functions of the MoM.

The radiation pattern, input impedance, VSWR, and gain are evaluated on the basis of the obtained current distribution. The positive direction of the current flow in Figs. 2, 5, and 9 corresponds to the direction from bottom to top on the vertical axis
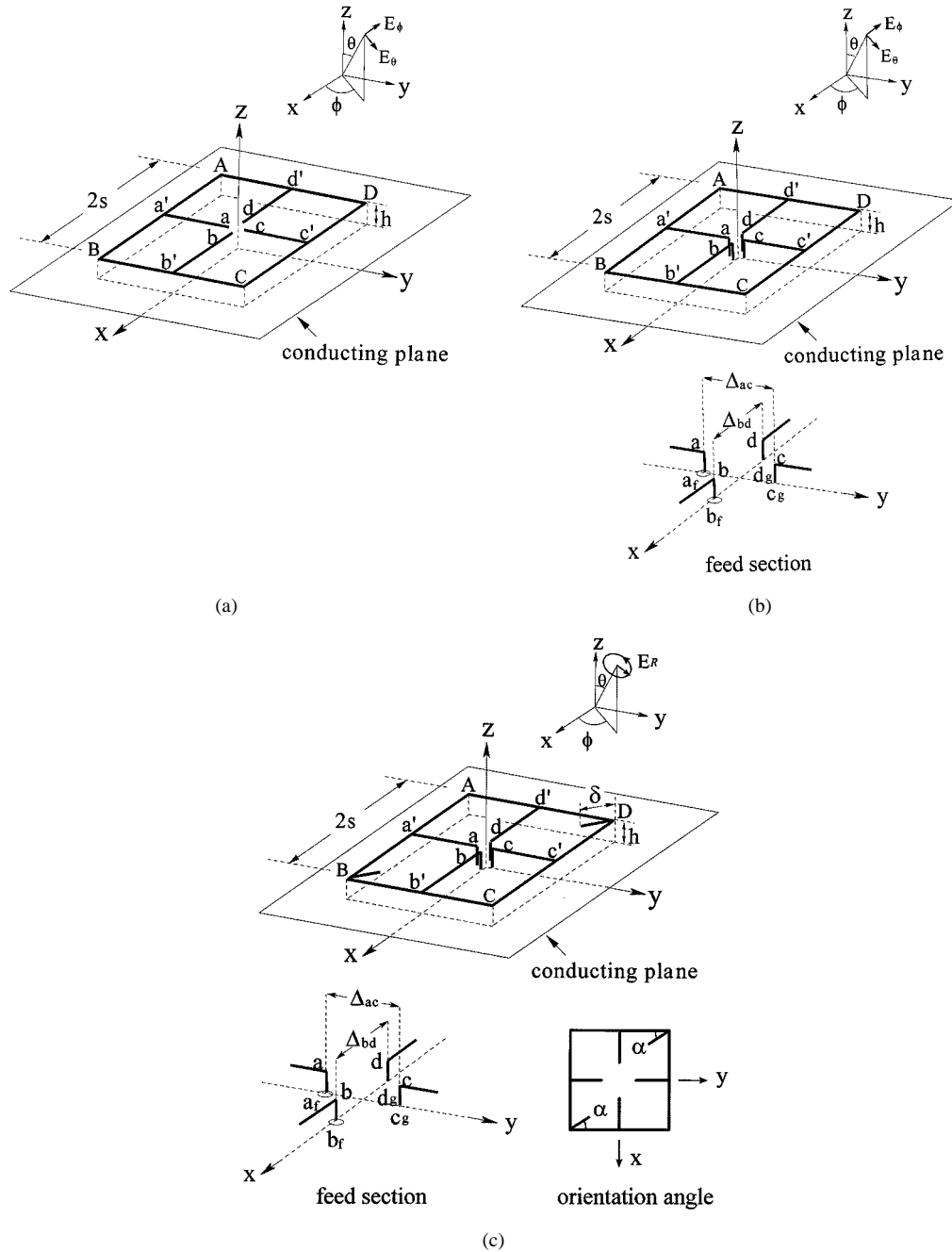
Fig. 1. Mesh antennas: (a) with balanced feed, MA-B; (b) with unbalanced feed, MA-U; either terminal a_f or b_f is used as the feed point; terminals c_g and d_g are in contact with the ground plane; and (c) with perturbation elements, MA-UP; either terminal a_f or b_f is used as the feed point; terminals c_g and d_g are in contact with the ground plane.

(where letters are used for representing the configuration) and left to right on the horizontal axis.

III. MESH ANTENNA WITH BALANCED FEED (MA-B)

The prototype of a mesh antenna for a radiation element of dual linear polarization is investigated in this section. Based on this prototype, two mesh antennas are constructed in Sections IV and V.

A. Configuration

Fig. 1(a) shows the configuration of an MA-B. The distance between the conducting plane and mesh (called the antenna height) is designated as h, and the mesh peripheral length for the square loop $ABCDA$ (where $AB = BC = CD = DA$) is designated as $8s$. The side lengths are chosen to be $Aa' = a'B = Bb' = b'C = Cc' = c'D = Dd' = d'A \equiv s$. The distance between terminals a and c is assumed to be infinitesimal (delta gap). The distance between terminals b and d is also assumed to be infinitesimal.

The antenna height for the MA-B is arbitrarily chosen: $h = 0.0635\lambda_0$. The peripheral length $8s$ of an MA-B with this height h is optimized such that the MA-B has an almost resistive impedance of 50 Ω at a test frequency of $f_0 = 4$ GHz, resulting in $8s = 1.272\lambda_0$.
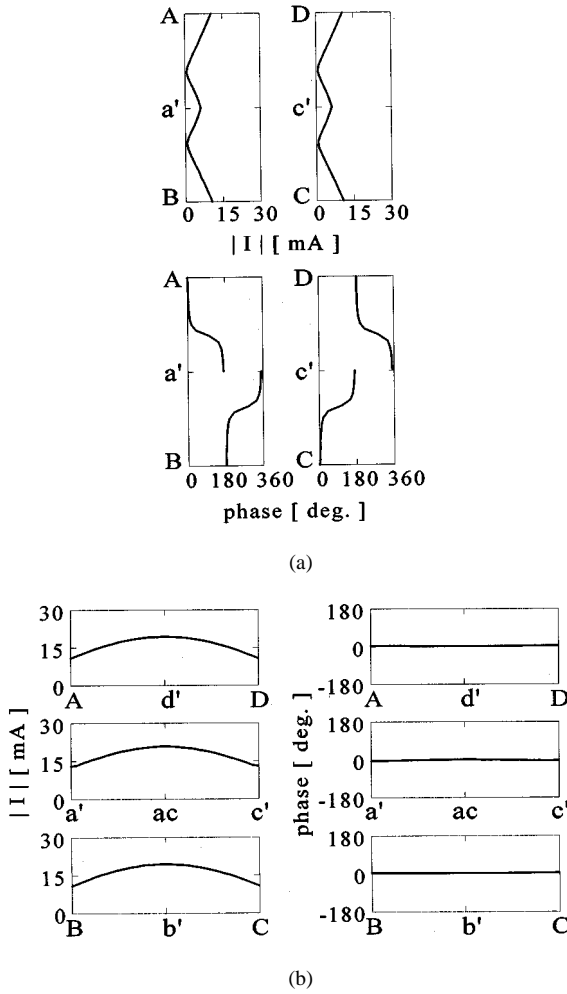
Fig. 2. Current distribution of the MA-B when terminals a and c are excited with a delta-gap source of 1 V and terminals b and d are open-circuited. Currents along the (a) x-directed wires and (b) y-directed wires.

B. Radiation Characteristics of MA-B

The MA-B is excited by a balanced feed. Let the terminals a and c be excited with a delta-gap source of 1 V and the terminals b and d be open. Fig. 2 shows the current distribution ($|I|$ is the amplitude of current $I = I_r + j I_i$). Note that the current does not flow along the x-directed center wires $b'b$ and $d'd$, and therefore Fig. 2 excludes the numerical results for the currents along these wires.

The currents along the x-directed wires Aa' and Ba' are symmetrical with respect to the junction point a' [see Fig. 2(a)]. Similarly, the currents along the x-directed wires Dc' and Cc' are symmetrical with respect to the junction point c'. These symmetrical currents lead to the cancellation of the radiation fields from all the x-directed wires (x-polarized radiation fields) in the z-direction.

The current distributions along the y-directed wires AD and BC have the same amplitude and phase [see Fig. 2(b)]. These are almost the same as the current distribution along the y-directed center wire $a'a$-cc' that has the source point. It follows that the radiation fields of y-polarization due to these three currents add in the z-direction, forming the radiation pattern shown in Fig. 3(a). The half-power beam width (HPBW) of the copolar-
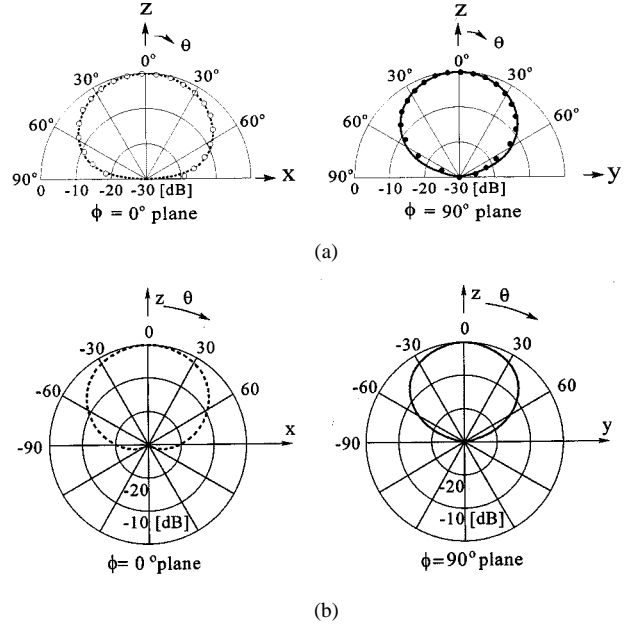

Fig. 3. Radiation pattern of the MA-B when terminals a and c are excited and terminals b and d are open-circuited. (a) In the $\phi = 0°$ and 90° planes for a ground plane of infinite extent. (b) In the $\phi = 0°$ and 90° planes for a finite-size ground plane of $2\lambda_0 \times 2\lambda_0$. theoretical E_θ —, measured E_θ • • •, theoretical E_ϕ —, and measured E_ϕ ∘ ∘ ∘.

ization component is approximately 75° in the $\phi = 0°$ plane (in the x-z plane) and 63° in the $\phi = 90°$ plane (in the y-z plane). Cross-polarization components do not appear in either plane. The measured radiation patterns (white dots for E_ϕ and black dots for E_θ), which are presented in Fig. 3(a), agree with the theoretical results. For the measurement, a large ground plane of $12\lambda_0 \times 12\lambda_0$ is used to approximate a theoretical ground plane of infinite extent. Note that the measurements performed throughout this paper use this ground plane. (Preliminary calculations for a finite-size ground plane using the finite-difference time-domain method [10]–[12] show that the radiation pattern and input impedance are not significantly affected when the size of the ground plane is larger than approximately $2\lambda_0 \times 2\lambda_0$. For reference, the theoretical radiation pattern for a ground plane of approximately $2\lambda_0 \times 2\lambda_0$ is shown in Fig. 3(b). Also, note that the present mesh antenna is supported by a honeycomb material spacer with a relative permittivity of $\varepsilon_r \approx 1$, as mentioned in Section II, and hence the effects of surface waves on the radiation characteristics can be neglected, unlike antennas printed on a dielectric substrate with $\varepsilon_r > 1$.)

Further calculations reveal that the frequency bandwidth for a VSWR = 2 (relative to 50 Ω) criterion is approximately 3%. The gain over this bandwidth is approximately 9.5 dB.

The above-mentioned results have been obtained under the condition that terminals a and c are excited and terminals b and d are open. Points to be noted are that there is no current flowing along the x-directed center wires $b'b$ and $d'd$ and the radiation is linearly y-polarized with no cross-polarization component. Since the antenna has a symmetrical configuration with respect to the mesh center point, when terminals a and c are open and terminals b and d are excited, as opposed to the previous case, the radiation is linearly x-polarized. The same VSWR and gain characteristics as those for the y-polarization are reproduced for
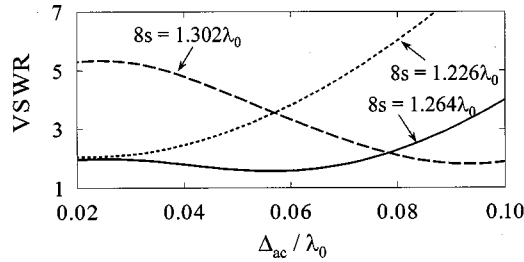
Fig. 4.   VSWR of the MA-U as a function of the distance between the feed points Δ_{ac}.

the x-polarization. In other words, the MA-B can be used as a radiation element of dual linear polarization by switching the feed.

IV. MESH ANTENNA WITH UNBALANCED FEED (MA-U)

Although not illustrated in Fig. 1(a), the MA-B in the previous section requires balun circuits to realize a balanced feed. To avoid the complexity of using balun circuits for the feed, a modified mesh antenna, which is fed from coaxial lines without balun circuits, is proposed and analyzed in this section.

A. Configuration

As shown in Fig. 1(b), the mesh antenna is modified to have four vertical wires $a_f a, b_f b, c_g c$, and $d_g d$. Either terminal a_f or b_f can used as a feed point. The other terminals c_g and d_g are in contact with the ground plane (short-circuited). The distance between terminals a_f and c_g (or a and c), Δ_{ac}, is chosen to be the same as that between terminals b_f and d_g (or b and d), Δ_{bd}. This antenna is distinguished from the previous MA-B and designated as the MA-U. It should be emphasized that the MA-U has a simpler feed system than the MA-B.

For comparison, the antenna height h of the MA-U is chosen to be the same as that for the previous MA-B: $h = 0.0635\lambda_0$. The MA-U is optimized to have an input impedance of approximately 50 Ω at a test frequency of $f_0 = 4$ GHz, as in the MA-B. This is performed by changing the distance between the feed points $\Delta_{ac} (= \Delta_{bd})$. Fig. 4 shows the VSWR (relative to 50 Ω) as a function of Δ_{ac} for three different loop peripheral lengths: $8s = 1.264\lambda_0$ and $1.264\lambda_0 \times (1 \pm 0.03)$. Based on this calculation, $\Delta_{ac} = 0.06\lambda_0$ and $8s = 1.264\lambda_0$ are adopted in the following calculations. Note that the optimized loop peripheral length of the MA-U is very close to that for the MA-B.

B. Radiation Characteristics of MA-U

The MA-U shown in Fig. 1(b) is analyzed under the condition that terminal a_f is excited and terminal b_f is open-circuited. The obtained current distribution is shown in Fig. 5. The currents along the x-directed wires $b'b$ and dd' are very small, as shown in Fig. 5(a). Therefore, it can be said that the situation observed in the previous MA-B (that is, the currents along the x-directed wires $b'b$ and dd' are zero) is approximately reproduced in the MA-U. This contributes to reducing the cross-polarization component in the radiation pattern.
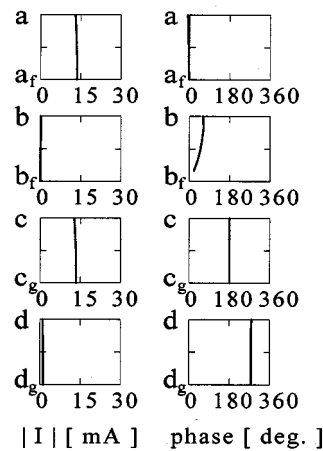
Fig. 6(a) and (b) shows the radiation patterns in the $\phi = 0°$ and $\phi = 90°$ planes, respectively. The measured data (white
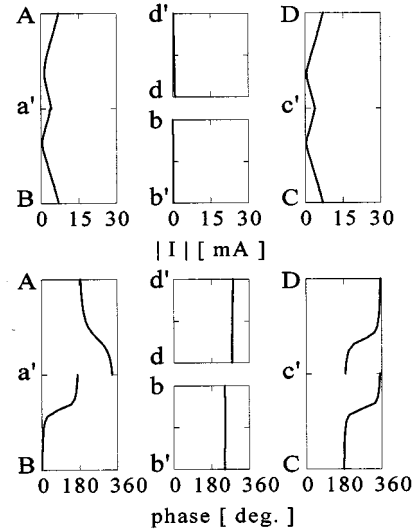
(a)
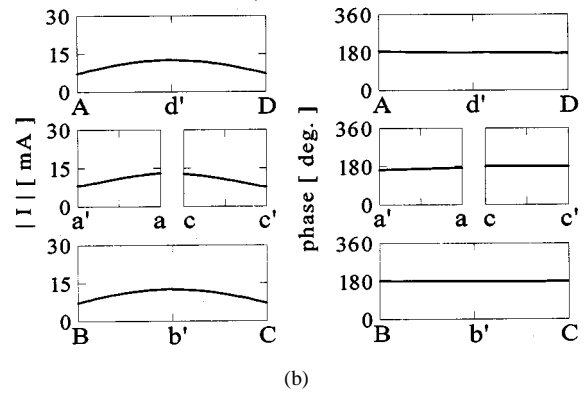
(b)

(c)

Fig. 5.   Current distribution of the MA-U when terminal a_f is excited and terminal b_f is open-circuited. Current amplitudes and phases along the (a) x-directed wires, (b) y-directed wires, and (c) z-directed wires.

dots for E_ϕ and black dots for E_θ) are also presented in these figures, showing good agreement with theoretical values.

In the $\phi = 0°$ plane, E_ϕ (dashed line) is the copolarization component and E_θ (solid line) is the cross-polarization component, as shown in Fig. 6(a). The copolarization component
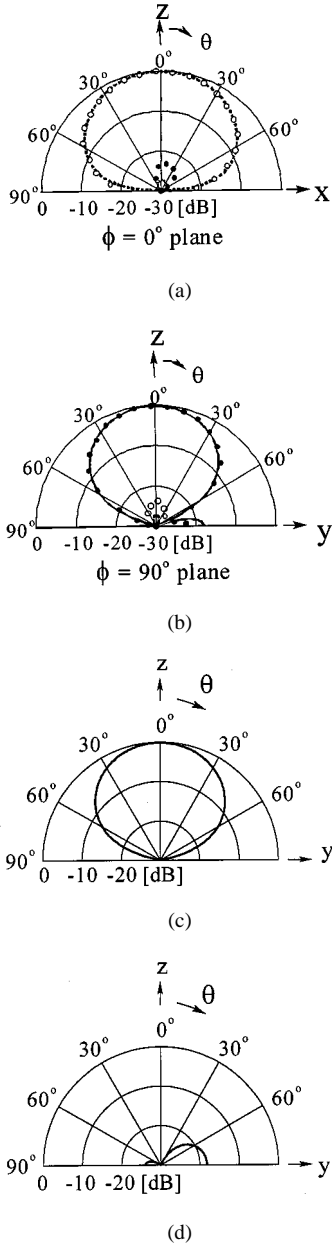
(a)

(b)

(c)

(d)

Fig. 6. Radiation pattern of the MA-U when terminal a_f is excited and terminal b_f is open-circuited. (a) Total radiation pattern in the $\phi = 0°$ plane, (b) total radiation pattern in the $\phi = 90°$ plane, (c) local radiation component E_θ from y-directed wires AD, $a'a$-cc', and BC, calculated in the $\phi = 90°$ plane, (d) local radiation component E_θ from z-directed wires $a_f a$, $b_f b$, $c_g c$, and $d_g d$, calculated in the $\phi = 90°$ plane. Theoretical E_θ —, measured E_θ ● ● ●, theoretical E_ϕ —, and measured E_ϕ ○ ○ ○.

E_ϕ is generated from the currents along the y-directed wires AD, $a'a$-cc', and BC, which are almost in-phase, as shown in Fig. 5(b). The cross-polarization component E_θ in the $\phi = 0°$ plane is generated from the currents along the x-directed wires BA, $b'b$, dd', and CD [see Fig. 5(a)] and z-directed wires $a_f a$, $b_f b$, $c_g c$, and $d_g d$ [see Fig. 5(c)]. The cross-polarization component is desirably low (theoretical value: -27 dB on the z-axis), as expected from the current phase relationships.

In the $\phi = 90°$ plane, E_θ (solid line) is the copolarization component and E_ϕ (dashed line) is the cross-polarization component, as shown in Fig. 6(b). Note that the currents along the
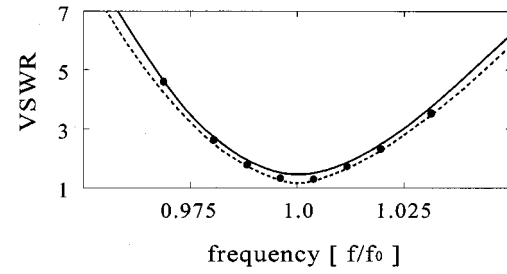

Fig. 7. Frequency response of the VSWR; theoretical (MA-U) - - -, measured (MA-U) ● ● ●, theoretical (MA-B) - - -. The MA-U is excited from terminal a_f with terminal b_f open-circuited.
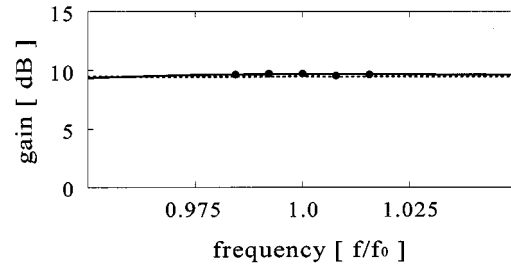

Fig. 8. Frequency response for the gain; theoretical (MA-U) —, measured (MA-U) ● ● ●, theoretical (MA-B) - - -. The MA-U is excited from terminal a_f with terminal b_f open-circuited.

y- and the z-directed wires generate the copolarization component E_θ in the $\phi = 90°$ plane. The E_θ shown in Fig. 6(b) can be decomposed into two local radiation components: the radiation from the y-directed wires [see Fig. 6(c), calculated using Fig. 5(b)] and the radiation from the z-directed wires $a_f a$, $b_f b$, $c_g c$, and $d_g d$ [see Fig. 6(d), calculated using Fig. 5(c)]. It is found that the currents along the z-directed wires slightly affect the symmetry of the radiation pattern in Fig. 6(c) produced by the currents along the y-directed wires, resulting in a small lobe near the y-axis, as shown in Fig. 6(b).

The small cross-polarization component E_ϕ in the $\phi = 90°$ plane appears due to the fact that the currents along the x-directed wires BA, $b'b$-dd', and CD are not perfectly symmetrical with respect to their middle points, as shown in Fig. 5(a). The amplitude values of the currents at symmetrical points with respect to the middle point of each x-directed wire are not identical (although they are almost the same), and a phase difference of exactly 180° is not obtained at these symmetrical points (although a phase difference of approximately 180° is obtained), as shown in Fig. 5(a).

The HPBW of the copolarization component is approximately 74° in the $\phi = 0°$ plane and 60° in the $\phi = 90°$ plane. Note that these HPBWs are close to those of the MA-B.

The frequency responses of the VSWR and gain are presented in Figs. 7 and 8, respectively, together with measured values (black dots). For comparison, the VSWR and gain of the MA-B are included (illustrated by dashed lines). It is clear that the MA-U has almost the same performances as the MA-B. The frequency bandwidth for a VSWR $= 2$ criterion is calculated to be approximately 3% with a maximum gain of 9.7 dB.

The results shown above have been obtained under the condition that terminal a_f is excited and terminal b_f is open-circuited, to obtain a linearly y-polarized wave. When terminal a_f is open-circuited and terminal b_f is excited, the antenna radiates a linearly x-polarized wave, reproducing the same VSWR and gain characteristics as those for the y-polarization. Thus, the MA-U is a radiation element of dual linear polarization, whose polarization can be switched by switching the feed point.

V. MA-U with Perturbation Elements (MA-UP)

So far, mesh antennas for dual linear polarization have been discussed. Now, a mesh antenna for dual circular polarization is investigated.

A. Configuration

When the MA-U shown in Fig. 1(b) is simultaneously excited from the two terminals a_f and b_f with equal amplitude and a $90°$ phase difference (this two-terminal simultaneous excitation is realized by using phase-delay circuits or phase shifters), the MA-U radiates a circularly polarized wave. In this section, single-terminal excitation of either a_f or b_f without any phase shifters, which is an obviously simpler excitation than the two-terminal simultaneous excitation, is considered to obtain a circularly polarized wave. For this, two perturbation elements [6], [13] are added to the MA-U, as shown in Fig. 1(c), where perturbation elements are specified by length δ and orientation angle α. This antenna is designated as MA-UP.

Throughout the following Sections V-B and -C, the distance between the feed points Δ_{ac} $(= \Delta_{bd})$ and the antenna height h are taken to be the same as those of MA-U in Section IV ($\Delta_{ac} = \Delta_{bd} = 0.06\lambda_0$ and $h = 0.0635\lambda_0$). The mesh peripheral length $8s$, perturbation element length δ, and orientation angle α are changed subject to the objectives of the analysis.

B. Radiation Characteristics of MA-UP

The mesh peripheral length $8s$, perturbation element length δ, and orientation angle α are fixed: $8s = 1.264\lambda_0$ (same as for MA-U), $\delta = 0.06\lambda_0 \equiv \delta_0$, and $\alpha = 45°$. Preliminary calculations reveal that when terminal a_f is excited and terminal b_f is *open-circuited*, MA-UP has standing-wave current distributions similar to those for MA-U, shown in Fig. 5. The perturbation elements in this case do not contribute to generating a traveling-wave current along the mesh periphery $ABCDA$. In other words, MA-UP with terminal b_f *open-circuited* cannot radiate a circularly polarized wave. Based on this fact, terminal b_f is connected to the ground plane in the following discussions.

Fig. 9(a) shows the current amplitude $|I|$ and phase along the mesh periphery $ABCDA$ when the minimum axial ratio is obtained at a relative frequency of $f/f_0 = 0.984$. The discontinuity points in the amplitude correspond to the wire branch points, where Kirchhoff's current law is satisfied. The variation in the amplitude is small (6 mA ± 1.57 mA). The phase changes by $360°$ along the periphery $ABCDA$. The local radiation from the periphery, therefore, contributes to generating a circularly polarized wave (a right-hand CP wave), as shown in Fig. 10(a). Note that the solid line in Fig. 10 shows the right-hand circularly polarized wave component of the radiation field E_R and
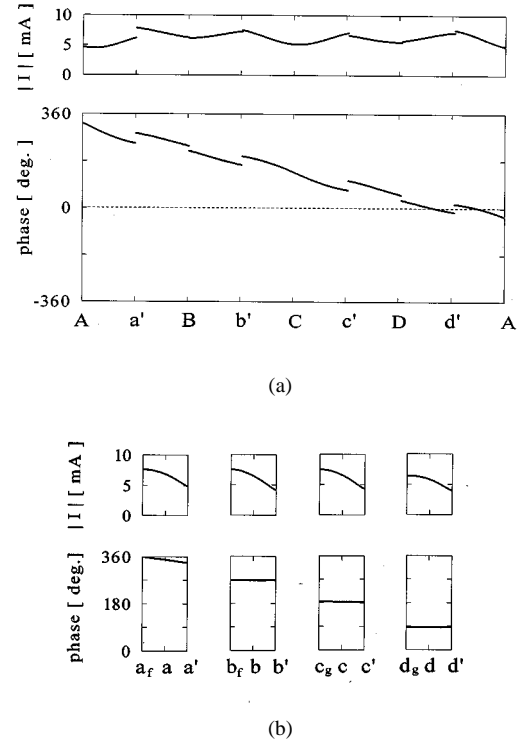

(a)

(b)

Fig. 9. Current distribution of the MA-UP; $8s = 1.264\lambda_0$, $\delta = 0.06\lambda_0$, and $\alpha = 45°$. Terminal a_f is excited with terminal b_f grounded. (a) Current amplitude and phase along mesh periphery $ABCDA$. (b) Current amplitudes and phases along the wires inside the mesh periphery $ABCDA$.

the dashed line shows the left-hand circularly polarized wave component E_L (cross-polarization component).

The current amplitude and phase along the four wires inside the periphery $ABCDA$ are shown in Fig. 9(b). These currents indicate almost the same amplitude with an approximately $-90°$ phase progression (the phase difference between the currents along neighboring wires is approximately $90°$). It follows that these currents radiate a circularly polarized wave (a right-hand CP wave), as shown in Fig. 10(b). Thus, the total radiation field [Fig. 10(a) plus (b)] is also circularly polarized, as shown in Fig. 10(c).

The dashed line in Fig. 11 shows the frequency response of the axial ratio. The frequency bandwidth for a 3-dB axial ratio criterion is approximately 1%. It is possible to shift the frequency ($f/f_0 = 0.984$) for the minimum axial ratio to the frequency $f_0(f/f_0 = 1)$ by slightly decreasing the peripheral length from $8s = 1.264\lambda_0$ to $1.240\lambda_0$. This is shown by a solid line in Fig. 11, which indicates almost the same 3-dB axial ratio bandwidth (approximately 1%). The measured results are also presented with black dots. Within this 3-dB axial ratio bandwidth for a decreased peripheral length of $8s = 1.240\lambda_0$, the theoretical VSWR shows values of less than 1.3 (see the dashed line in Fig. 12) with a theoretical gain of approximately 9.5 dB (see the dashed line in Fig. 13). This gain is very close to those for the MA-B and MA-U. Note that the theoretical VSWR and gain agree with measured results illustrated by black dots.

The above-mentioned radiation characteristics for right-hand circular polarization have been obtained when terminal a_f is excited and terminal b_f is grounded. With the opposite excita-
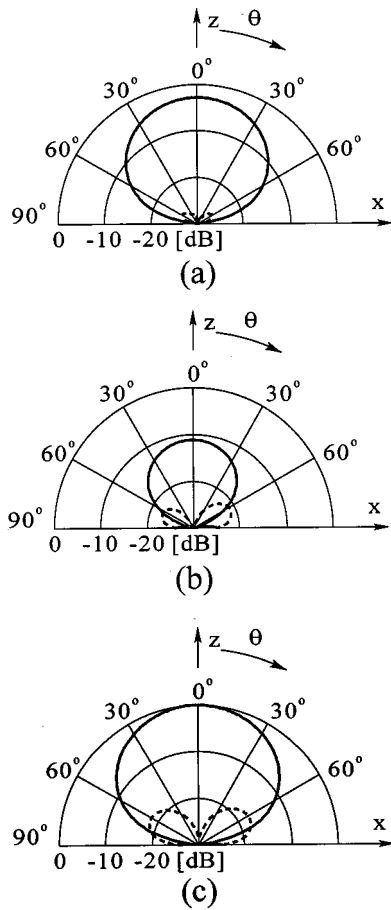
(a)

(b)

(c)

Fig. 10.   Radiation pattern of the MA-UP in the $\phi = 0°$ plane; $8s = 1.264\lambda_0$, $\delta = 0.06\lambda_0$, and $\alpha = 45°$. Terminal a_f is excited with terminal b_f grounded. Theoretical E_R —, theoretical E_L - - -. (a) Local radiation from mesh periphery $ABCDA$ with perturbation elements. (b) Local radiation from wires inside mesh periphery $ABCDA$. (c) Total radiation pattern.
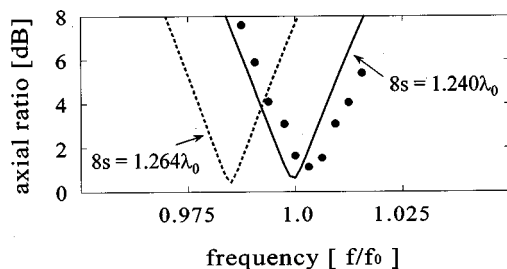

Fig. 11.   Frequency response for the axial ratio of the MA-UP; $\delta = 0.06\lambda_0$ and $\alpha = 45°$. Terminal a_f is excited with terminal b_f grounded. Theoretical $(8s = 1.264\lambda_0)$ - - -, theoretical $(8s = 1.240\lambda_0)$ —, measured $(8s = 1.240\lambda_0)$ • • • • •.

tion (terminal b_f is excited and terminal a_f is grounded), the MA-UP can radiate a left-hand circularly polarized wave with the same frequency responses for the axial ratio, VSWR, and gain, as shown in Figs. 11–13, respectively. This means that the MA-UP acts as a radiation element of dual circular polarization.

C. *Effects of Perturbation Elements*

To investigate the effects of the perturbation elements on the antenna characteristics, the mesh peripheral length is fixed to
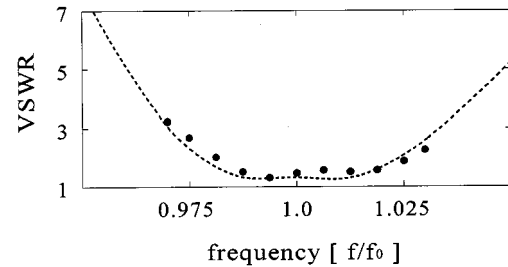

Fig. 12.   Frequency response for the VSWR of the MA-UP; $8s = 1.240\lambda_0$, $\delta = 0.06\lambda_0$, and $\alpha = 45°$. Terminal a_f is excited with terminal b_f grounded. Theoretical - - -, measured • • •.

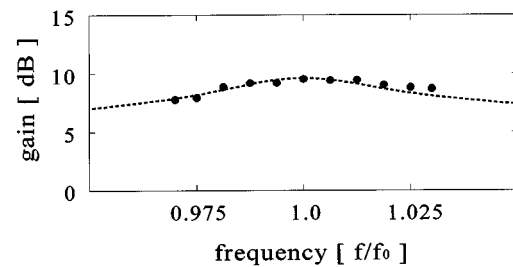

Fig. 13.   Frequency response for the gain of the MA-UP; $8s = 1.240\lambda_0$, $\delta = 0.06\lambda_0$, and $\alpha = 45°$. Terminal a_f is excited with terminal b_f grounded. Theoretical - - -, measured • • •.
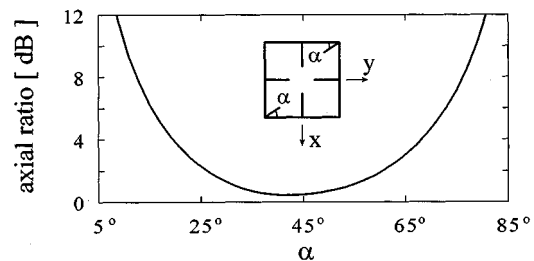

Fig. 14.   Axial ratio of the MA-UP as a function of orientation angle α; $8s = 1.240\lambda_0$ and $\delta = 0.06\lambda_0$. Terminal a_f is excited with terminal b_f grounded.

be $8s = 1.240\lambda_0$ (used in Figs. 11–13), and the perturbation element length δ and orientation angle α are changed.

Fig. 14 shows the axial ratio as a function of the orientation angle α of the perturbation elements, each having a length of $\delta = \delta_0$ ($= 0.06\lambda_0$, which has been used in Section V-B). It is found that the best orientation angle for radiation of circular polarization is $\alpha = 45°$. Note that this value has also been used in Section V-B. In the following analyses, an orientation angle of $\alpha = 45°$ is used.

Fig. 15 shows the changes in the gain and VSWR for a right-hand circularly polarized wave when the perturbation element length is made longer $(\delta_L = \delta_0 + 0.02\lambda_0)$ and shorter $(\delta_S = \delta_0 - 0.02\lambda_0)$ than the initial value $\delta_0 = 0.06\lambda_0$. Two facts are revealed as the perturbation element length increases: 1) the frequency at which the gain shows a maximum value becomes lower and 2) the VSWR in the lower frequency region improves. Fig. 16 shows the axial ratios for these two perturbation element lengths δ_L and δ_S as a function of frequency,
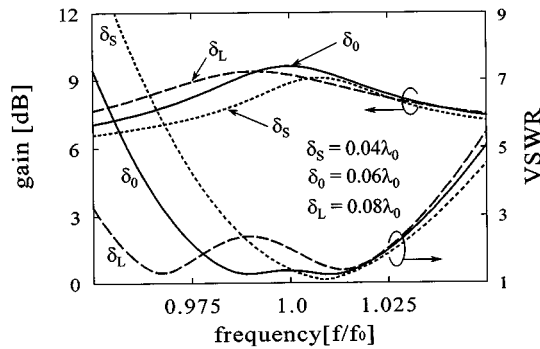
Fig. 15. Frequency responses for the gain and VSWR of the MA-UP; $8s = 1.240\lambda_0$ and $\alpha = 45°$. Terminal a_f is excited with terminal b_f grounded.
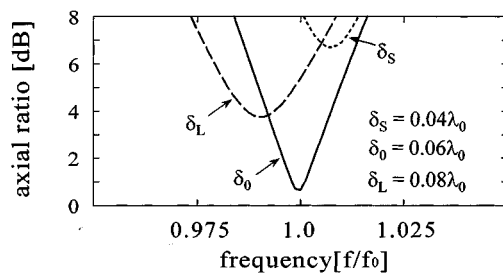

Fig. 16. Frequency response for the axial ratio of the MA-UP; $8s = 1.240\lambda_0$ and $\alpha = 45°$. Terminal a_f is excited with terminal b_f grounded.

together with that for δ_0. It can be said that the frequency at which the axial ratio shows a minimum value becomes lower as the perturbation element length increases.

VI. CONCLUSION

The radiation characteristics of three mesh antennas (MA-B, MA-U, and MA-UP), including the radiation pattern, gain, and VSWR, have been calculated on the basis of the current distributions obtained by using the method of moments.

The MA-B is fed from the middle point of a y-directed center wire. The three currents along the y-directed wires have almost the same amplitude and phase. In this case, currents along the x-directed center wires do not exist. Thus, the polarization of the radiation is in the y-direction. By virtue of the symmetrical configuration with respect to the antenna center point, a linearly x-polarized wave is also obtained by switching the feed point.

The MA-U is a modified version of the MA-B. The four terminals of the MA-B are reduced to two for the MA-U. The advantage of the MA-U is that a dual linearly polarized wave can be obtained with a simplified feed system. The analysis reveals that the cross-polarization component is desirably low (-27 dB on the z-axis). The HPBW of the copolarization component is approximately $74°$ in the $\phi = 0°$ plane and $60°$ in the $90°$ plane, which are close to those of the MA-B. The MA-U has almost the same frequency responses for the VSWR and gain as the MA-B.

The MA-UP, which is an extension of the MA-U, is proposed as a radiation element of dual circular polarization. The MA-UP has two perturbation elements to obtain a traveling-wave current along the mesh periphery. It has been revealed that both the mesh periphery and the four wires inside the mesh periphery generate

circularly polarized waves. The frequency bandwidth for a 3-dB axial ratio criterion is approximately 1% for an extremely low antenna height of $0.0635\lambda_0$. Within this bandwidth, the VSWR shows values of less than 1.3 with a gain of approximately 9.5 dB. This gain is close to those of the MA-B and MA-U.

REFERENCES

[1] R. C. Johnson and H. Jasik, *Antenna Engineering Handbook*, 3rd ed. New York: McGraw-Hill, 1993, vol. 43, ch. 5.
[2] *Antenna Handbook*, Y. T. Lo and S. W. Lee, Eds., Van Nostrand Reinhold, New York, 1988. "Wire and loop antennas".
[3] C. A. Balanis, *Antenna Theory*. New York: Harper and Row, 1982, ch. 5.
[4] T. Tsukiji, "Characteristics of twin rectangular loop antennas and complex loop antennas," , IEICE Rep. AP87-43, June 1987.
[5] H. Nakano, K. Hirose, T. Suzuki, S. R. Kerner, and N. G. Alexopoulos, "Numerical analyzes of printed line antennas," in *Proc. Inst. Elect. Eng.*, vol. 136, Apr. 1989, pp. 98–104.
[6] H. Nakano, "A numerical approach to line antennas printed on dielectric materials," in *Computer Physics Communications* Amsterdam, the Netherlands, Aug. 1991, vol. 68, pp. 441–450.
[7] R. F. Harrington, *Field Computation by Moment Methods*. New York: Macmillan, 1968.
[8] A. F. Peterson, S. L. Ray, and R. Mittra, *Computational Methods for Electromagnetics*. Piscataway, NJ: IEEE Press, 1998, pp. 190–196.
[9] H. Nakano, "Antenna analysis using integral equations," in *Analysis Methods for Electromagnetic Wave Problems*, E. Yamashita, Ed. Boston, MA: Artech House, 1996, vol. II, ch. 3.
[10] K. S. Yee, "Numerical solution of initial boundary value problems involving Maxwell's equations in isotropic media," *IEEE Trans. Antennas Propagat.*, vol. AP-14, pp. 302–307, May 1966.
[11] A. Taflove, *Computational Electrodynamics: The Finite-Difference Time Domain Method*. Norwood, MA: Artech House, 1995.
[12] Z. P. Liao, H. L. Wong, B. P. Yang, and Y. F. Yuan, "A transmitting boundary for transient wave analyzes," *Sci. Sinica*, ser. A, vol. 27, no. 10, pp. 1063–1076, 1984.
[13] H. Nakano, H. Yoshida, H. Mimaki, J. Yamauchi, and K. Hirose, "Printed loop array antenna radiating a circularly polarized wave," in *Proc. 9th Int. Conf. Antennas and Propagation (ICAP)*, the Netherlands, Apr. 1995, pp. 504–507.

H. Nakano (M'75–SM'87–F'92) was born in Ibaraki, Japan. He received the B.E., M.E., and Dr.E. degrees in electrical engineering from Hosei University, Tokyo, in 1968, 1970, and 1974, respectively.

Since 1973, he has been a Member of the Faculty of Hosei University, where he is now a Professor of electronic informatics. His research topics include numerical methods for antennas, electromagnetic wave scattering problems, and lightwave problems. He has published more than 160 refereed journal papers and 120 international symposium papers on antenna and relevant problems. He is the author of *Helical and Spiral Antennas* (New York: Research Studies Press, 1987). He published the chapter "Antenna Analysis Using Integral Equations" in *Analysis Methods of Electromagnetic Wave Problems*, vol. 2 (Norwood, MA: Artech House, 1996). He was a Visiting Associate Professor at Syracuse University, Syracuse, NY, during March–September 1981, a Visiting Professor at the University of Manitoba, Canada, during March–September 1986, and a Visiting Professor at the University of California, Los Angeles, during September 1986–March 1987.

Dr. Nakano received an International Scientific Exchange Award from the Natural Sciences and Engineering Research Council of Canada in 1986. In 1987, he received the Best Paper Award from the Institute of Electrical Engineers 5th International Conference on Antennas and Propagation. In 1994, he received the IEEE AP-S Best Application Paper Award (H. A. Wheeler Award). He is an Associate Editor of IEEE ANTENNAS AND PROPAGATION MAGAZINE and was a member of the AP-S administrative committee in 2000.

N. Suzuki was born in Tokyo, Japan, on February 27, 1975. She received the B.E. and M.E. degrees from Hosei University, Tokyo, Japan, in 1997 and 1999, respectively.

She joined the Matsushita Communication Industrial Company Ltd., Tokyo, in 1999.

Ms. Suzuki is a member of the Institute of Electronics, Information and Communication Engineers of Japan.

J. Yamauchi (M'85) was born in Nagoya, Japan, on August 23, 1953. He received the B.E., M.E., and Dr.E. degrees from Hosei University, Tokyo, Japan, in 1976, 1978, and 1982, respectively.

From 1984 to 1988, he was a Lecturer in the Electrical Engineering Department of Tokyo Metropolitan Technical College. Since 1988, he has been a Member of the Faculty of Hosei University, where he is now a Professor of electronic informatics. His research interests include optical waveguides and circularly polarized antennas.

Dr. Yamauchi is a member of the Optical Society of America and the Institute of Electronics, Information and Communication Engineers of Japan.

T. Ishii was born in Kanagawa, Japan, on October 16, 1976. He received the B.E. degree in electrical engineering from Hosei University, Tokyo, Japan, in 1999, where he is currently pursuing the M.E. degree.

He is a member of the Institute of Electronics, Information and Communication Engineers of Japan.